Appl. Phys. A 81, 1053–1057 (2005)
DOI: 10.1007/s00339-004-2945-y

Applied Physics A
Materials Science & Processing

S.V.M. DE MORAES[1]
M.T. LARANJO[1]
M. ZAT[1]
T.M.H. COSTA[1]
M.R. GALLAS[2]
E.V. BENVENUTTI[1,✉]

High-pressure effects on nanometric hybrid xerogels, *p*-phenylenediamine/silica and *p*-anisidine/silica

[1] LSS, Instituto de Química, UFRGS, CP 15003, 91501-970, Porto Alegre, RS, Brazil
[2] LAPMA, Instituto de Física, UFRGS, CP 15051, 91501-970, Porto Alegre, RS, Brazil

Received: 16 March 2004/Accepted: 31 May 2004
Published online: 29 July 2004 •

ABSTRACT The hybrid xerogels *p*-phenylenediamine/silica and *p*-anisidine/silica were prepared with different surface areas and porosities and they were processed at high pressure (7.7 GPa or ∼ 76 000 atm) in a quasi-hydrostatic medium at room temperature. The morphologies of the materials were studied before and after the high-pressure treatment by using N_2 adsorption–desorption isotherms, scanning electron microscopy and infrared thermal analysis. The porous hybrid *p*-phenylenediamine/silica presented after the high-pressure treatment a surface-area reduction and an entrapment of organics in closed pores. However, the less porous hybrid *p*-anisidine/silica showed a surprising behavior, a pressure-induced increase in surface area with opening of pores. We propose a mechanism based on the inhibition of the cold sintering process by the organics to explain these results.

PACS 81.20.-n; 81.40.Vw; 81.05.-t

1 Introduction

The sol–gel method is an attractive route to prepare several silica-based materials, with promising properties that allow their potential application as sorbents, sensors, catalysts and optical and electrochemical devices [1–8]. The sol–gel method to prepare silica consists basically in the hydrolysis (Scheme 1) and polycondensation of alkoxysilanes in tetraethylorthosilicate (TEOS) or tetramethylorthosilicate (TMOS) (Schemes 2a and 2b) that result in a cross-linked silica network [9].

$$\mathrm{Si(OR)_4 + H_2O \rightarrow (RO)_3Si{-}OH + ROH} \quad (1)$$

$$\equiv \mathrm{SiOH + OH{-}Si} \equiv \rightarrow \equiv \mathrm{Si{-}O{-}Si} \equiv + \mathrm{H_2O} \quad (2a)$$

$$\equiv \mathrm{Si{-}OH + RO{-}Si} \equiv \rightarrow \equiv \mathrm{Si{-}O{-}Si} \equiv + \mathrm{ROH} \quad (2b)$$

Thus, it is possible to insert several organic groups in the silica structure by choosing an appropriate organosilane ($\mathrm{R{-}Si(OR)_3}$) to be hydrolyzed and polycondensed simultaneously with the TEOS or TMOS. The resulting hybrid materials present a very stable organic phase [10, 11].

The high-pressure technique is an effective tool to be used for compaction of silica-based powder materials, improving mechanical, optical and morphological properties [12–16]. Costa et al. [17] proposed a cold sintering mechanism to explain the compaction of a pure silica system at room temperature. The high-pressure compaction produces an approach of silanol groups that react to form bridged siloxanes, resulting in a more cross-linked and compacted silica network. In this process the pure silica undergoes a drastic reduction in the surface area, near 100 times, due to the formation of a microstructure with closed pores.

In the present work, the high-pressure technique was used to compact, at room temperature, the hybrid-based silica, *p*-phenylenediamine/silica (*p*-PhAS/silica) and *p*-anisidine/silica (*p*-ANS/silica). The high-pressure effects on silica-containing organics were investigated by using infrared spectroscopy, N_2 adsorption–desorption isotherms and scanning electron microscopy.

2 Experimental

2.1 *Synthesis*

For the synthesis of the sol–gel organic precursors the *p*-phenylenediamine and *p*-anisidine were activated with sodium hydride in 10 ml of aprotic solvents mixture (toluene:thf) (Merck) (1:1) for 30 min, and 3-chloropropyltrimethoxysilane (CPTMS, Merck) was added. The quantities used were stoichiometric (5 mmol) for *p*-phenylenediamine (Merck), *p*-anisidine, CPTMS and NaH (Acros). The mixtures were stirred under argon at solvent-reflux temperature for a period of 5 h. The solutions were then centrifuged, and the supernatants that contain the *p*-phenylenediaminepropyltrimethoxysilane (*p*-PhAS) or *p*-anisidinepropyltrimethoxysilane (*p*-ANS) were used as sol–gel organic precursors in the two gelation processes. Afterwards, tetraethylorthosilicate (TEOS, Acros) (5 ml), ethyl alcohol (Merck) (5 ml), HF (0.1 ml, Synth) and water in stoichiometric ratio with Si $r = 4/1$ (1.6 ml) were added to the precursor solutions, under stirring. The gelations occur by a fluoride nucleophilic catalytic process, at pH ∼ 10. The mixtures were stored for a week, just covered without sealing, for gelation and solvent evaporation. The resulting xerogels were then extensively washed using the following solvents: toluene, thf, ethyl alcohol, distilled water and ethyl ether. The xerogels were finally dried for 30 min in an oven at 100 °C. The resulting xerogel powders were designated *p*-PhAS/silica and *p*-ANS/silica.

✉ Fax: +55-51/3316-7304, E-mail: edilson@iq.ufrgs.br

2.2 *High-pressure technique*

For the high-pressure technique, the xerogel powders were initially pre-compacted in a piston–cylinder-type die to approximately 0.1 GPa. The volume of pre-compacted samples was about 0.35 cm^3 (diameter of 8 mm and height of 7 mm). The samples were then placed in a Pb container which acted as a quasi-hydrostatic pressure-transmitting medium. The high-pressure processing was accomplished in a toroidal-type chamber at 7.7 ± 0.5 GPa ($\sim 76\,000$ atm) at room temperature [18]. The pressure calibration was accomplished by the fixed-points method [19].

2.3 *Infrared analysis*

Self-supporting disks of the materials were prepared, with an area of 5 cm^2, weighing ~ 100 mg. The disks were heated in a temperature range from 100 to 450 °C under vacuum (10^{-2} Torr, 1 Torr = 133.3 Pa), for 1 h. The infrared cell used in this work was described elsewhere [20]. The equipment used was a Shimadzu Fourier-transform infrared (FTIR) spectrometer, model 8300. The spectra were obtained with a resolution of 4 cm^{-1}, with 100 scans.

2.4 N_2 *isotherms*

The nitrogen adsorption–desorption isotherms of previously degassed solids, at 150 °C, were determined at liquid-nitrogen boiling point in a home-made volumetric apparatus, with a vacuum-line system employing a turbomolecular Edwards vacuum pump. The pressure measurements were made using a capillary Hg barometer. The specific surface areas of the hybrid materials were determined using the BET (Brunauer, Emmett and Teller) [21] multipoint method and the pore-size distribution was obtained using the BJH (Barret, Joyner and Halenda) method [22].

2.5 *Scanning electron microscopy*

The hybrid xerogel materials were analyzed with a Jeol model JSM 5800 scanning electron microscope (SEM), with 20 kV and 60 000 times magnification.

3 Results and discussion

The synthesis of the sol–gel organic precursors employing a SN_2 reaction between 3-chloropropyltrimethoxysilane (CPTMS) and aromatic amines has been described by using sodium hydride as a base activator [23]. The organic precursors *p*-PhAS and *p*-ANS, synthesized in this work, are illustrated in Fig. 1.

In the presence of tetraethylorthosilicate (TEOS), water and HF catalyst, the organic precursors undergo hydrolysis and polycondensation. The resulting hybrid xerogel materials present a covalent organic–inorganic interface, and the organics can be dispersed in open pores or trapped in closed pores [11].

Infrared thermal analysis is a very effective tool to investigate the presence and the distribution of the organic phase in hybrid xerogel materials with a covalent organic–inorganic interface. The analysis is based on the evolution of the infrared band areas of the organics in relation to the thermal treatment [11]. The band area of the organics dispersed in open pores, when covalently bonded, is almost constant up to 300 °C. However, these organics are completely desorbed when heat treated up to 450 °C, in vacuum. The remaining organic bands that do not vanish are attributed to trapped organics in closed pores [11]. Thus, it is possible to calculate the relative organic coverage, i.e. organic groups that are really on the surface, in open pores. This is obtained by subtracting the band areas corresponding to the organic trapped groups from the band areas of the organic total content. The organic band-area values are obtained by using the overtone silica band at ~ 1870 cm^{-1} as a reference band. This normalization was necessary, considering the heterogeneity in the disk's thickness, so as to take into account the position changes of the infrared beam.

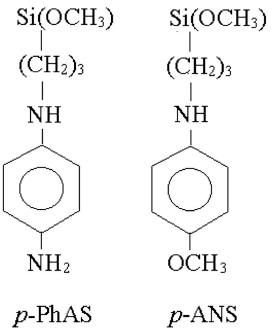

FIGURE 1 Sol–gel organic precursors used

The infrared spectra of the *p*-PhAS/silica and *p*-ANS/silica materials are presented in Figs. 2 and 3, respectively. The great organic thermal stability observed for the powdered samples heat treated up to 400 °C, in the vacuum cell, is evidence that these groups are strongly bonded to the surface in the covalent form. It is possible to observe that the fraction of organics that remained in the powdered

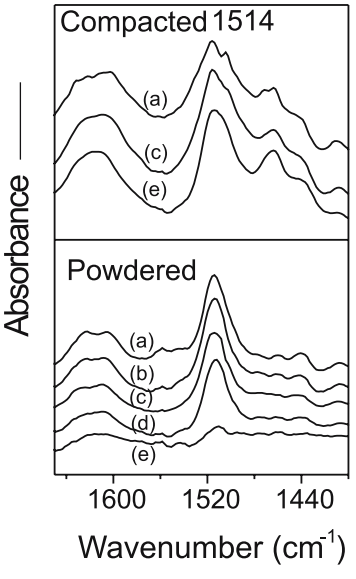

FIGURE 2 Infrared spectra of powdered and compacted (7.7 GPa) *p*-PhAS/silica samples, obtained after heat treatment in vacuum for 1 h up to: (a) 100; (b) 200; (c) 300; (d) 400 and (e) 450 °C. The bar value is 0.5 for both powdered and compacted samples

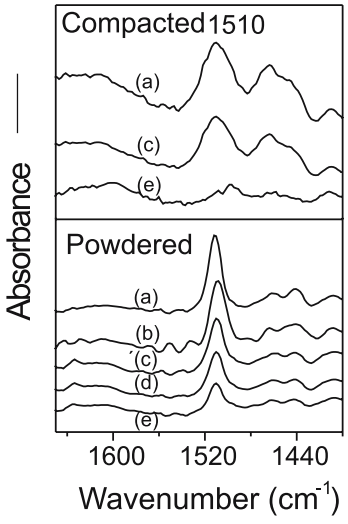

FIGURE 3 Infrared spectra of powdered and compacted (7.7 GPa) *p*-ANS/silica samples, obtained after heat treatment in vacuum for 1 h up to: (a) 100; (b) 200; (c) 300; (d) 400 and (e) 450 °C. The bar value is 0.5 and 0.2 for powdered and compacted samples, respectively

p-ANS/silica material, even after heat treatment up to 450 °C, is 57% (Table 1), higher than the fraction observed for the *p*-PhAS/silica material, which is only 10%. The relative remaining organic grade indicates the presence of organics in closed pores [11]. Therefore, the powdered *p*-ANS/silica material presents a larger fraction of organic groups trapped in closed pores than the powdered *p*-PhAS/silica material. These results are in agreement with the surface-area and pore-volume measurements presented in Table 1. The surface-area and pore-volume values of the powdered *p*-ANS/silica material are lower (near 40%) than the values for the powdered *p*-PhAS/silica material.

The infrared spectra of the *p*-PhAS/silica and *p*-ANS/silica compacted samples at 7.7 GPa are also shown in Figs. 2 and 3, respectively. It is possible to observe that the high-pressure processing closed some existing pores for *p*-PhAS/silica material, since the relative remaining organic grade, estimated from the spectra of the samples heat treated up to 450 °C, increased from 10 to 77% after applying the high pressure (Table 1). Confirming these results, the surface area and pore volume of the compacted *p*-PhAS/silica sample also decreased from 175 to 65 $m^2\,g^{-1}$ and from 0.30 to 0.07 $cm^3\,g^{-1}$, respectively (Table 1). For the compacted *p*-ANS/silica sample, the relative remaining organic grade of 25% was lower than that obtained for the powdered sample, which was 57% (Table 1), indicating that, for this sample, the high-pressure processing, surprisingly, promoted the opening of pores and this fact made possible the organics liberation during the thermal treatment, in the vacuum cell. These results are also confirmed by surface-area data that show a higher value for this sample after the high-pressure processing. The *p*-ANS/silica results are unexpected if compared with that obtained for pure silica gel [17] and even for a *p*-PhAS/silica sample.

The pore size distribution curves, obtained from the N_2 desorption isotherms, are presented in Fig. 4. It is possible to observe that the *p*-PhAS/silica material presents a higher porosity than the powdered *p*-ANS/silica material. The high-pressure processing produces a closing of the pores for *p*-PhAS/silica material; on the other hand, no measurable effect can be detected for the *p*-ANS/silica material.

Costa et al. [17] reported that when pure silica gel is submitted to similar high-pressure values, the surface area undergoes a drastic reduction, decreasing from 300 to 3 $m^2\,g^{-1}$. This effect was interpreted as a consequence of the surface dehydroxylation, i.e. conversion of silanol to siloxane groups, induced by the higher silanol proximity in the compacted samples [17]. In the present work, for the porous *p*-PhAS/silica that is a hybrid material, the closing of the pores was not too impressive, since after the high-pressure processing, the surface area and pore volume decrease by about 50% (Table 1), but even so a fraction of open pores remained. In this case, the surface pendant organic groups prevented the complete reaction between the silanol groups, hindering the cold sintering process, as represented in Fig. 5.

On the other hand, for the *p*-ANS/silica hybrid material, which presents a very low porosity even in the powdered form, the changes were totally unexpected. The high-pressure pro-

Sample	Thermal treatment/ °C	IR band area/ Abs.cm^{-1} (Relative remaining organic grade/%)	Surface area/$m^2\,g^{-1}$	Pore volume/ $cm^3\,g^{-1}$
Powdered p-PhAS/ silica	100	2.1 (100)	175	0.30
	200	2.1 (100)		
	300	2.1 (100)		
	400	2.0 (95)		
	450	0.2 (10)		
Compacted p-PhAS/ silica	150	2.2 (100)	65	0.07
	300	2.2 (100)		
	450	1.7 (77)		
Powdered p-ANS/ silica	100	2.1 (100)	65	0.13
	200	2.1 (100)		
	300	1.7 (81)		
	350	1.6 (76)		
	450	1.2 (57)		
Compacted p-ANS/ silica	150	1.6 (100)	90	0.08
	300	1.2 (75)		
	450	0.4 (25)		

TABLE 1 Infrared band areas of aromatic ring stretching and porosity data of hybrid materials

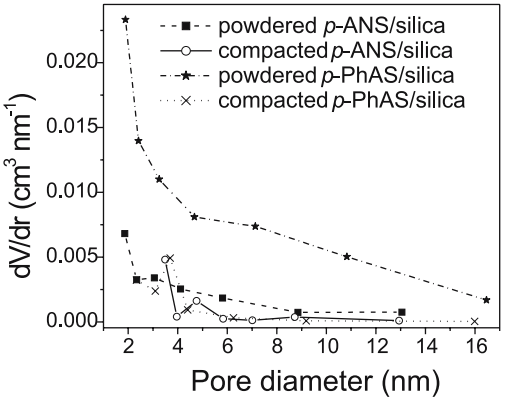

FIGURE 4 Pore-size distribution of the *p*-PhAS/silica and *p*-ANS/silica hybrid materials, powdered and compacted at 7.7 GPa

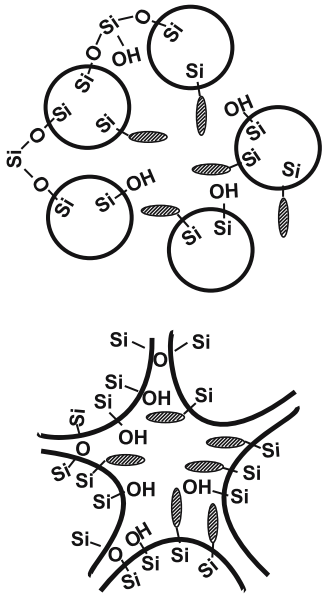

FIGURE 5 Model for the structure effects in a cold sintering process in the presence of the organics

cessing produced an increase in the surface area (see Table 1), which is confirmed by a lower remaining organic grade as already explained.

In general, when we apply high pressure to powdered samples, using a quasi-hydrostatic transmitting medium, the energy is dissipated in a sample-volume reduction, with a decrease of porosity, or in phase transitions [24–26]. For the

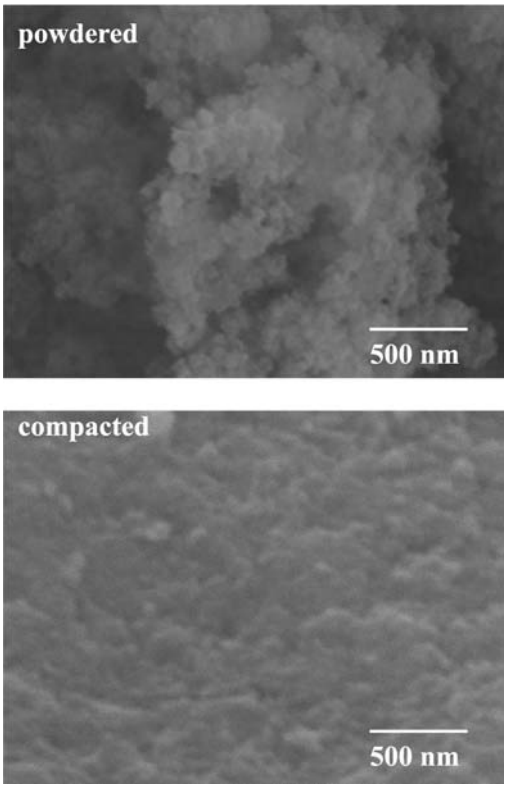

FIGURE 6 SEM images of *p*-PhAS/silica hybrid material, powdered and compacted at 7.7 GPa. The magnification was 60 000 times

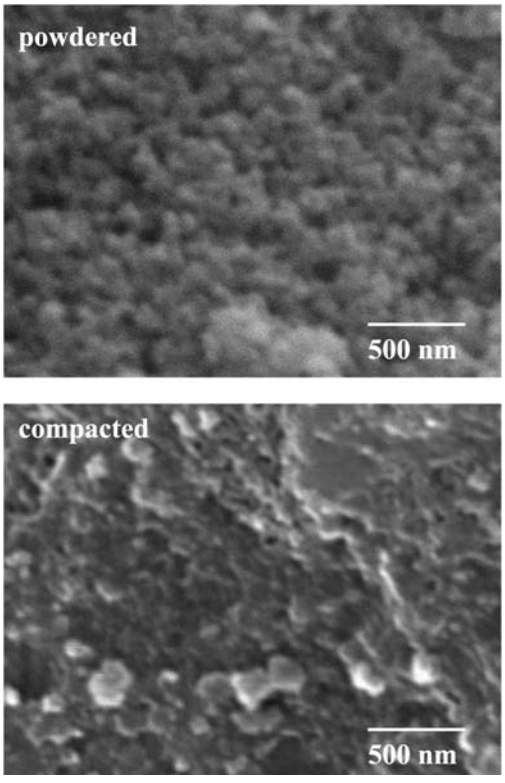

FIGURE 7 SEM images of *p*-ANS/silica hybrid material, powdered and compacted at 7.7 GPa. The magnification was 60 000 times

p-PhAS/silica, a porous sample, the energy dissipation occurred by the reduction of porosity; however, this process was not so impressive as already observed for pure silica [17], due to the presence of organics. For the powdered *p*-ANS/silica hybrid, this kind of dissipation process could be hindered because this material has a relatively lower porosity even in the powdered form (Table 1 and Fig. 4) and, additionally, presents surface organic groups. Therefore, the energy dissipation in *p*-ANS/silica material could happen by a shearing process between particles, causing microstructural defects formed at the onset of plastic deformation in the particles.

The SEM images obtained for *p*-PhAS/silica and *p*-ANS/silica hybrid materials that are shown in Figs. 6 and 7, respectively, confirm the above propositions. The decrease of the porosity for *p*-PhAS/silica material is evident after applying the high pressure. However, for the *p*-ANS/silica, the reduction of porosity is not clearly observed; the samples were very similar in this respect. The compacted samples showed a platelet microstructure that could confirm the hypothesis of the dissipation of energy by shearing or plastic deformation of particles.

4 Conclusions

The porous powdered *p*-PhAS/silica hybrid material, when submitted to high pressure, undergoes a surface-area and porosity reduction with consequent entrapment of organics in closed pores. This effect was not so impressive when compared to pure silica, and it could be explained considering that the surface organic groups partially hinder the cold sintering process. On the other hand, for the less porous

powdered *p*-ANS/silica hybrid material, the high pressure produces an amazing increase in surface area with an opening of the pores, observed by the liberation of the organics after the heat treatment, in a vacuum cell. This behavior was interpreted considering that the energy applied during the high-pressure processing is dissipated by shearing between the particles, causing the opening of the pores.

ACKNOWLEDGEMENTS We thank FAPERGS (Fundação de Amparoà Pesquisa no Estado do Rio Grande do Sul, Brasil) and CNPq (Conselho Nacional de Desenvolvimento Científico e Tecnológico, Brasil) for financial support and grants. We also thank the CME-UFRGS for the use of the SEM.

REFERENCES

1 O. Lev, Z. Wu, S. Bharathi, V. Glezer, A. Modestov, J. Gun, L. Rabinovich, S. Sampath: Chem. Mater. **9**, 2354 (1997)
2 Z. Lu, E. Lindner, H.A. Mayer: Chem. Rev. **102**, 3543 (2002)
3 W. Que, Y. Zhou, Y.L. Lam, Y.C. Chan, C.H. Kam: Appl. Phys. A **73**, 171 (2001)
4 M.M. Collinson: Trends Anal. Chem. **21**, 30 (2002)
5 P. Yang, C.F. Song, M.K. Lu, G.J. Zhou, D. Xu, D.R. Yuan: Appl. Phys. A **74**, 689 (2002)
6 T. Salesch, S. Bachmann, S. Brugger, R. Rabelo-Schaefer, K. Albert, S. Steinbrecher, E. Plies, A. Mehdi, C. Reye, R.J.P. Corriu, E. Lindner: Adv. Funct. Mater. **12**, 134 (2002)
7 S.V.M. de Moraes, J.B. Passos, P. Schossler, E.B. Caramão, C.C. Moro, T.M.H. Costa, E.V. Benvenutti: Talanta **59**, 1039 (2003)
8 F.A. Pavan, T.M.H. Costa, E.V. Benvenutti: Colloids Surf. A **226**, 95 (2003)
9 D.A. Loy, K.J. Shea: Chem. Rev. **95**, 1431 (1995)
10 L.T. Arenas, T.A.S. Aguirre, A. Langaro, Y. Gushikem, E.V. Benvenutti, T.M.H. Costa: Polymer **44**, 5521 (2003)
11 F.A. Pavan, S.A. Gobbi, T.M.H. Costa, E.V. Benvenutti: J. Therm. Anal. Calorim. **68**, 199 (2002)
12 M.R. Gallas, A.R. Rosa, T.M.H. Costa, J.A.H. da Jornada: J. Mater. Res. **12**, 764 (1997)
13 T.M.H. Costa, V. Stefani, N. Balzaretti, L.T.S.T. Francisco, M.R. Gallas, J.A.H. da Jornada: J. Non-Cryst. Solids **221**, 157 (1997)
14 T.M.H. Costa, M.R. Gallas, E.V. Benvenutti, J.A.H. da Jornada: J. Phys. Chem. B **103**, 4278 (1999)
15 E. Ol'khovik, O. Figovsky, V. Feigin: Mater. Res. Innov. **2**, 115 (1998)
16 M.A. Springuel-Huet, J.L. Bonardet, A. Gédéon, Y. Yue, V.N. Romannikov, J. Fraissard: Micropor. Mesopor. Mater. **44–45**, 775 (2001)
17 T.M.H. Costa, M.R. Gallas, E.V. Benvenutti, J.A.H. da Jornada: J. Non-Cryst. Solids **220**, 195 (1997)
18 L.G. Khvostantsev: High Temp. High Pressures **16**, 171 (1984)
19 W.F. Sherman, A.A. Stadmuller: *Experimental Techniques and High-pressure Research* (Wiley, New York 1987)
20 J.L. Foschiera, T.M. Pizzolato, E.V. Benvenutti: J. Braz. Chem. Soc. **12**, 159 (2001)
21 S. Brunauer, P.H. Emmett, E. Teller: J. Am. Chem. Soc. **60**, 309 (1938)
22 E.P. Barret, L.G. Joyner, P.P. Halenda: J. Am. Chem. Soc. **73**, 373 (1951)
23 F.A. Pavan, S. Leal, Y. Gushikem, T.M.H. Costa, E.V. Benvenutti: J. Sol–Gel Sci. Technol. **23**, 129 (2002)
24 A. Jayaraman: Sci. Am. **250**, 54 (1984)
25 L. Spain, P. Bolsaitis: *Phase Transformation at High Pressure* (Marcel Dekker, New York 1977)
26 S.N. Achary, G.D. Mukherjee, A.K. Tyagi, S.N. Vaidya: J. Mater. Sci. **37**, 2501 (2002)